BUDAPEST UNIVERSITY OF TECHNOLOGY AND ECONOMICS

FACULTY OF MECHANICAL ENGINEERING

DEPARTMENT OF POLYMER ENGINEERING

ÁDÁM STOCKER

SSC PAPER

THE EFFECT OF INTERLEAF FILMS ON THE OUT-OF-PLANE LOAD-BEARING AND DAMAGE TOLERANCE OF HIGH-PERFORMANCE COMPOSITES

Thesis leader:

Dr Gergely Czél

associate professor

BUDAPEST, 2023

LIST OF CONTENTS

1. INTRODUCTION

Currently, there is an ever-growing demand for high-performance materials that are strong and tough but light at the same time. Carbon fibre-based composite materials have proven to be one of the best materials for achieving high strength at low density. They are among the leading options for the material of weight-critical vehicles, sports equipment, and engineering structures. The main way of producing composite materials is to embed high-strength fibres in a tough polymeric matrix. At the high end of these polymeric composites, pre-impregnated (prepreg) fibre sheets have one of the highest fibre contents.

The development of new technologies and improvement of materials is a challenge for many and require continuous research. Although carbon fibre composites have outstanding strength, they have limited toughness and damage tolerance due to the brittle behaviour of their constituents. Extensive research has been conducted on toughening composite materials and increasing their energy absorption upon impact. Delamination is one of the main reasons for sudden failure of composite laminates. In this case, the composite material cannot use the full strength of the fibres, and failure occurs between the plies in the weaker matrix material.

The project aimed to modify the most common quasi-isotropic plate configuration with suitable film interleaving for better overall interlaminar fracture toughness. I produced 16-ply quasi-isotropic S-glass fibre/epoxy prepreg laminates for the baseline specimens. Then I made a modified version where I placed a polytetrafluoroethylene (PTFE) release film to the mid-plane of the laminate.

The produced specimens were subjected to mechanical tests to study their out-of-plane load-bearing and damage tolerance. The test methods included quasi-static indentation tests to measure the damage resistance and compression after impact (CAI) tests to determine the residual compressive strength and damage tolerance.

2. LITERATURE REVIEW

2.1. Modifications of Prepreg Composite Structures

Marino et al. [1] produced polyamide 12 (PA12) film interleaved discontinuous carbon/epoxy – continuous glass/epoxy hybrid composites. They aimed to make the laminates more tolerant to damage by increasing their interlaminar toughness and to make the delamination damage repairable by heating. They developed a repair method which successfully restored the original pseudo-ductile behaviour of the tested laminates. The interleaving increased the interlaminar fracture toughness of the composite plates making them more damage tolerant.[1]

Cohades et al. [2] reported about extrinsic self-healing in fibre-reinforced polymer composite materials which is implemented by the addition of functional materials or architecture to the laminate. [2]

Marino et al. [3] produced poly(acrylonitrile-butadiene-styrene) (ABS) and polystyrene (PS) film interleaved carbon-glass/epoxy hybrid composites. They reported that the ABS interleaf had a toughening effect on the interfaces of the hybrid laminates and eliminated the stress drops observed during the tensile test in the tested unidirectional hybrid laminates without interleaf films. In the case of PS films, they found that after oxygen plasma treatment the mechanical performance of hybrid composites containing PS interleaves increased, creating toughening mechanisms leading to more stable delamination.
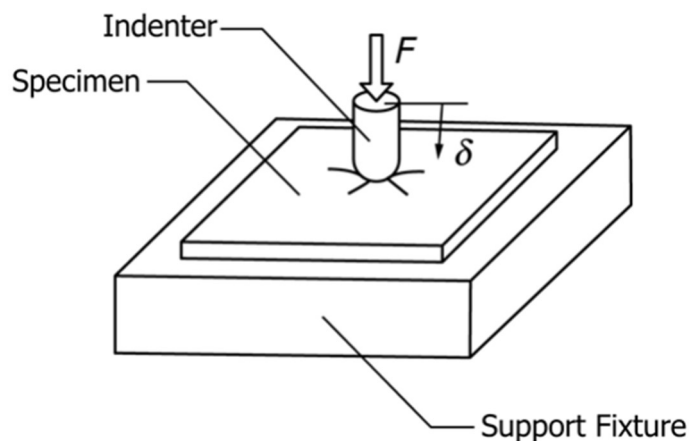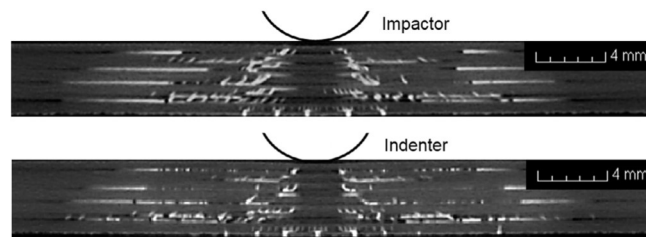
2.2. Concentrated Quasi-Static Indentation

Fig. 1. Quasi-static indentation test [4].

Concentrated quasi-static indentation (QSI) is a mechanical material test method. In the case of fibre-reinforced polymer-matrix composites, a flat, rectangular specimen plate is placed on a support fixture and subjected to an out-of-plane, concentrated force in the middle of the plate exerted by a hemispherical indenter pressed into the surface of the plate at low velocity. This test method may be used to screen and determine the

damage resistance properties of specimens which can be quantified by critical contact force. Another purpose may be to inflict a specific size and type of damage into the specimen for subsequent damage tolerance testing (e.g., compression after indentation test). [5]

An alternative method of creating damage by an out-of-plane concentrated force and measuring the damage resistance properties is the drop-weight impact test. However, due to the oscillation in the recorded force during the drop-weight impact test, the association of specific damage events with a specific quantity of force is often difficult. Furthermore, using impact tests, there is no option to interrupt the process during different stages of damage development to observe the succession and evolution of damage mechanisms within the plate. Upon a drop-weight impact test, only the final damage state is identifiable. Meanwhile, concentrated quasi-static indentation tests have been shown to result in similar global behaviour and damage states as low-velocity drop-weight impact tests [6]–[8]. This phenomenon is illustrated in Fig. 2. [4] which shows X-ray images comparing two identical composite laminates with inflicted damage by quasi-static indentation and low-velocity impact tests having no obvious difference in terms of damage morphology. [5],[4]

Fig. 2. X-ray images of cross-section of two identical Ps laminates (Ply-blocked

scaling) comparing damage extent caused by dynamic low-velocity impact (upper)

and quasi-static indentation (lower). [4]

Abisset et al. [4] performed a unique series of scaled indentation tests on quasi-isotropic composite plates. The tests were conducted with a 16 mm diameter indenter on an INSTRON servo-hydraulic testing machine. The support fixture was a cut-out configuration with a 125x75 mm window. The tests were conducted under displacement control with 0.5 mm/min speed of testing. The sampling rate of load and displacement was 20 Hz. To evaluate the repeatability of the test and determine the load level for each load drop, three specimens were loaded until total failure. Then, they loaded and interrupted one specimen immediately before the first significant drop in the load curve. They interrupted tests just after the first load drop. They also interrupted tests at different load levels between the first load drop and final specimen failure load. In this way, they provided a detailed set of results for both global behaviour and damage evolution to demonstrate the behaviour control mechanisms.

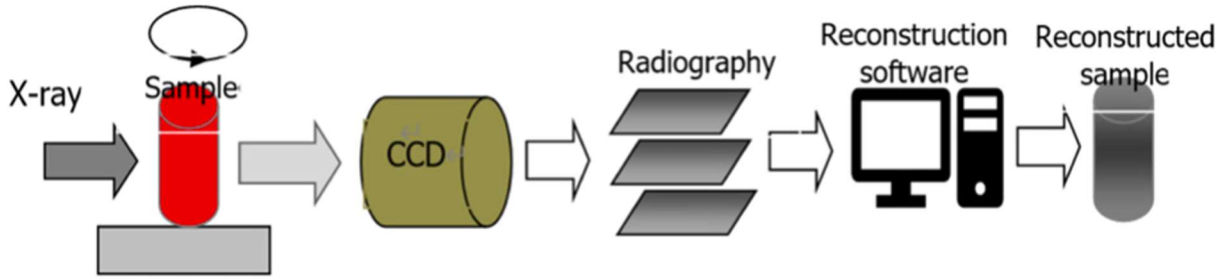## 2.3. Most common NDT methods to analyse delamination in composites

Fig. 3. Schematic illustration of the principle of X-ray computed tomography. [9]

X-ray computed tomography (X-CT) has become a powerful tool in material research. X-CT imaging has a broad range of applications in examining fibre reinforced composites. It can accurately depict the architecture of the constituent phases and provide insights into defects that may arise during manufacturing or accumulate during service. Its primary applications include modelling, assessing manufacturing processes, characterizing environmental conditions, and evaluating mechanical behaviours under loading. [9]
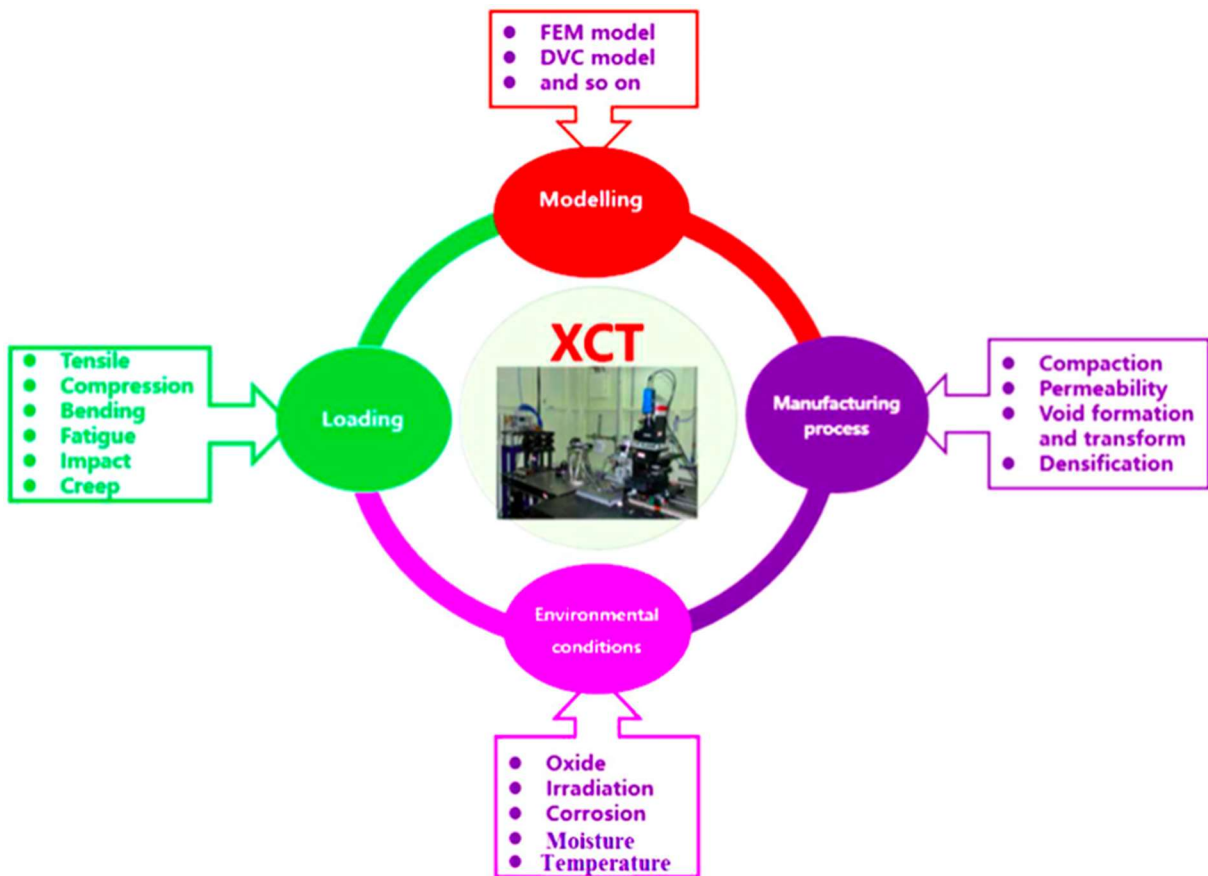

Fig. 4. Schematic representation of applications of X-ray computed tomography on fiber reinforced composites. [9]

Abisset et al. [4] used non-destructive techniques, including ultrasonic C-scan and X-ray Computer Tomography (CT), and carried out a detailed assessment of the damage evolution in quasi-isotropic composite plates which were tested with static indentation.

Bull et al. [10] monitored the internal damage development in three dimensions carried out by microfocus X-ray computed tomography (μCT). They took scans of carbon fibre coupons after the application of failure near-failure compression loads and after coupon failure carried out by compression after impact tests. They also conducted compression after impact tests and ultrasonic C-scans to complement the observations made from μCT scans and to investigate the effect of the projected damage area on the residual compressive strength.

Ultrasonic testing (C-scan) is a non-destructive technique used to identify faults in structural components. The technique encompasses various methods that are used to classify defects and evaluate them with high sensitivity, speed, and simplicity. Ultrasonic testing has been approved for use in a wide range of domains, including aerospace, automotive, composite testing, and transportation. With the progress made, new methods have been discovered and corrected, resulting in improved defect detection and various material properties. [11]
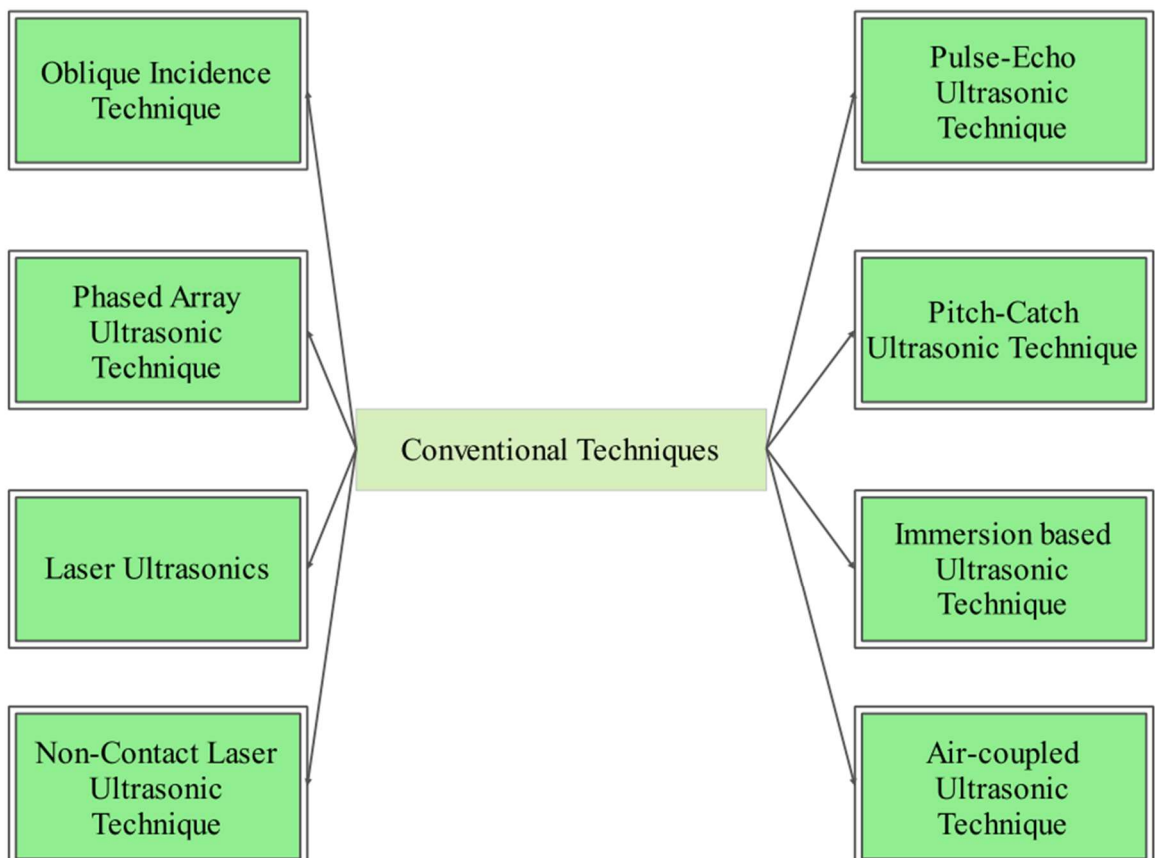
Fig. 5. Various Conventional Techniques of NDT. [11]

Various composite damage detection techniques utilizing different apparatus setups have been developed using ultrasound technology in either wave or pulse form. Each technique has its own advantages and disadvantages. [11]

Guinard et al. [12] developed an ultrasonic C-scan bench which enabled a thorough description of 3D damage and served as validation when comparing numerical results to experiments. They built a cinematic scheme based on ultrasonic scanning and distance magnitude analysis. They compared the size of the damaged area in the simulation to the measured maximal width of the ultrasonic C-scan and found matching results.

2.4. Compression After Indentation

The compressive residual strength properties of damaged polymer matrix composite plates can be investigated by the compression after indentation/impact mechanical material test method. A flat, rectangular composite plate is subjected to a damaging event (impact or static indentation). Then it is installed in a stabilization fixture, that has been aligned to minimize loading eccentricities and induced bending of the specimen. The assembly is placed between flat platens and loaded with compressive force until the failure of the specimen. The application of compressive force on the plates may happen after the quasi-static indentation test (compression after indentation) or after the impact test (compression after impact). [13]
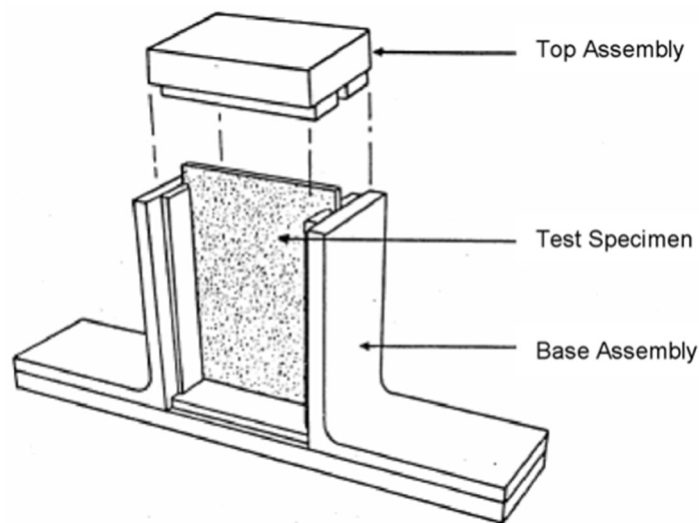

Fig. 6. Schematic of compressive residual strength support fixture with specimen in place [13].

Zhang et al. [14] studied the influence of two different positions of high-velocity impact (projectile penetration) conducted with compression after impact tests. They found that the centre impacted laminates had a failure mode of main buckling, the edge impact laminates had compression failure near the impact hole side and buckling failure near the centre of the laminate.

2.5. Summary

Interleaving have shown to improve damage tolerance by increasing interlaminar toughness. It is relatively easy to implement while it is highly cost-effective.

To examine the damage tolerance impact test methods are commonly used, however, this has its drawbacks. Noise in the force signal, not interruptible, only the final damage state is investigable, and several attempts are needed.

Quasi-static indentation has shown to result in similar behaviour and damage states as low-velocity impact tests. It is interruptible at different stages of damage evolution and may be used to inflict a specific size and type of damage. For good comparability with impact damage introduction, it may be beneficial to use a cut-out support fixture and a hemispherical indenter tip.

C-scans and CT scans are capable tools for analysing damage inside of composite laminates without further destruction. X-CT have shown to be well suited for evaluating damage introduced under loading.

Compression tests can be used to investigate residual strength properties of damaged composite laminates. In addition to the reasons mentioned above, it is also preferable in this case to use the static indentation test as to a damaging event and then perform compression after indentation tests.

3. EXPERIMENTAL

3.1. Aims and Purposes

The experimental work aimed to make changes to the interlaminar properties of the composite structure and then see how it affects the overall load bearing and damage tolerance. The purpose of the modification was to influence the role of the interfaces and make the delamination upon failure more controllable and stable. I aimed to modify the middle interlayer of the composite structure. My key consideration was, that the typical damage mode of quasi-isotropic (QI) composite plates under out of plane load is delamination at multiple interfaces. If I can concentrate the damage to the middle interface, better residual compressive strength could be obtained after damage, as two thick layers are stiffer than several thinner ones after delamination. The stiffer blocks can withstand global buckling typical of damaged plated under compression better.

3.2. Experimental Plan

The sequence of actions during the research study is summarised here:
- Produce:
    - Quasi-isotropic glass fibre/epoxy matrix laminates
    - Modified version of the laminates by placing polymer film interleaf to the middle interface
- Perform:
    - Quasi-static indentation tests (with cameras and backlight)
        - To introduce damage and assess the damage tolerance
        - To test the load bearing until final failure
        - Perform reloading tests to assess the effect of the introduced damage
    - Non-destructive tests
        - Preliminary X-CT scans
    - Compression after indentation tests (with cameras and backlight)
        - Assess the residual strength
- Evaluate:
    - Quasi-static indentation tests
    - Non-destructive tests
    - Compression after indentation tests
- Conclude

3.3. Materials

I used S-glass fibre/913 epoxy prepreg manufactured by Hexcel Corporation to make the test plates (Table 1, Table 2). I used 15 μm thick commercial PTFE) release films to modify the selected layer interfaces of the composite plates.

Table 1. Properties of the fibres in the prepreg.

	Fibre properties		
	Elastic modulus [GPa]	Failure strain [%]	Tensile strength [MPa]
OCV flitestrand S-glass	92	3.6-4.4	3300-4100

Table 2. Properties of the prepreg.

	Prepreg properties		
	Fibre volume fraction [%]	Nominal cured ply thickness [mm]	Estimated elastic modulus [GPa]
S-Glass/913 epoxy	49.4	0.25	47.1

3.4. Equipment

Autoclave

I used the Olmar ATC 1100/2000 type autoclave available at the laboratory to make the test plates from prepreg sheets. It has a 10-bar maximum internal pressure and 260°C maximum temperature. The number of internal vacuum connections is 2 and the internal thermocouples is 4.

Fig. 7. Olmar ATC 1100/2000 type autoclave [15].

Tensile Test machine

I used the Zwick Z250 type tensile tester with the 20 kN load cell for the static indentation tests and with the 250 kN load cell for the compression after indentation tests using the Zwick TestXpert II. Program. The tensile tester has a speed range of 0.001–600 mm/min and a load capacity of -250 – +250 kN.

Fig. 8. Zwick Z250 type tensile tester [15].

Static Indentation Support Fixture and Indenter

I used a support fixture for the quasi-static indentation test made according to the standard of the drop-weight impact test method (ASTM D7136/D7136M) [16]. The fixture base has a 75 x 125 mm rectangular cut-out and four toggle clamps attached. It also has three guiding pins 12.5 mm from the edges of the cut-out for positioning the specimens. I used an indenter with a 16 mm diameter hemispherical tip.
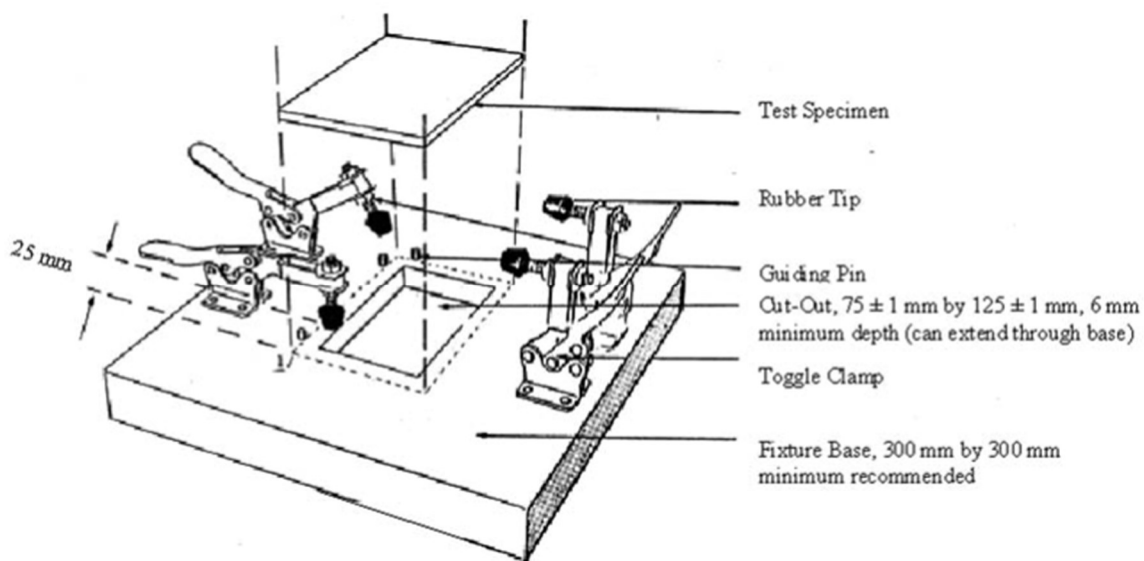

Fig. 9. Impact support fixture [16].

Compression After Impact Fixture

I used a compression after-impact support fixture made by Zwick Roell according to ASTM D7137/D7137M [11].


Fig. 10. Zwick Roell compression after impact support fixture [17].

3.5. Experimental Work

3.5.1. Fabrication of Test Specimens

The S-Glass/Epoxy prepreg roll first had to be taken out of the freezer, where it was stored at $-20°C$ to slow the cross-linking in the matrix. The roll was acclimatised at room temperature overnight. Then I cut 300x300 mm squares and isosceles right triangles with 300 mm sides. It was necessary to cut the triangles because the 300 mm width of the roll did not allow direct cutting of squares with 45° orientation. Two triangles connected at the hypotenuse would give a square. This way, the triangles were used to make plies with +/− 45° fibre direction. I laminated blocks made of 4 plies: [45/90/-45/0] and placed them in a vacuum bag to remove any residual air from the layers. I made a baseline laminate building together 4 blocks of 4 plies prepared previously to make a symmetric 16-ply laminate: $[45/90/-45/0]_{2s}$. I then made modified versions of this laminate, where I placed an interleaf between the two middle 0° plies. The interleaf was a 40 mm diameter circular piece of PTFE release film.
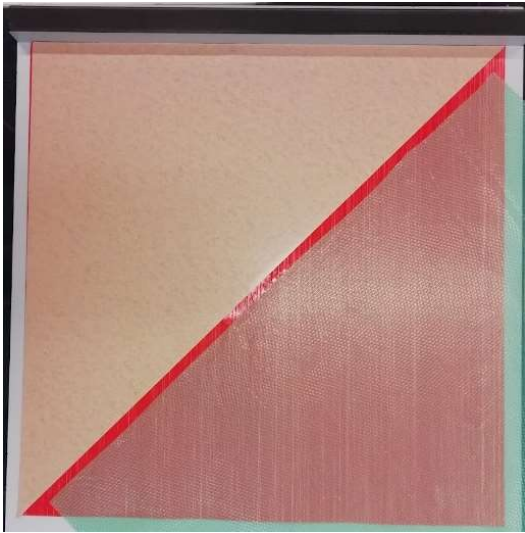
| **a)** Hand lay-up | **b)** Interleaf disc |
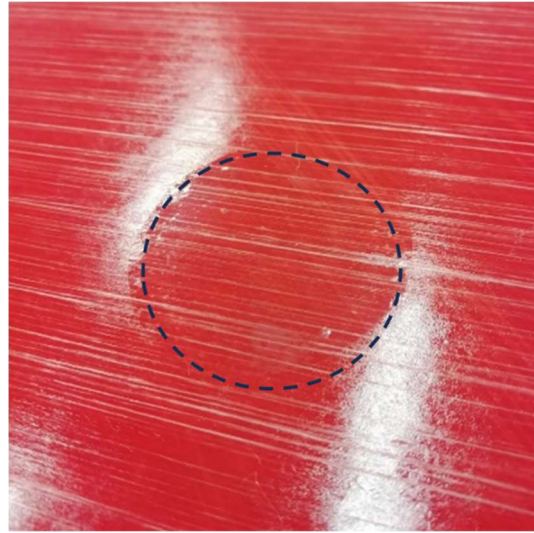
Fig. 11. Intermediate step in the manual lamination process **(a)** and interleaf disc at the middle interface **(b)**.

Then I built the vacuum bag for the laminates on an 8 mm thick flat aluminium (Al) tool plate. I started with the tool plate and attached the release film. Then I placed the laminates on the tool plate in contact with one another and built a silicone dam around the laminates to limit resin leakage and placed the 5 mm thick Al top plate on them. I then covered everything with breather mat and positioned the bases of vacuum valves. The tool plate and the product were covered with vacuum film and sealed with yellow heat-resistant vacuum sealant tape. I also made pleats to leave extra bagging material to prevent the stretching of the film around the edges and corners.
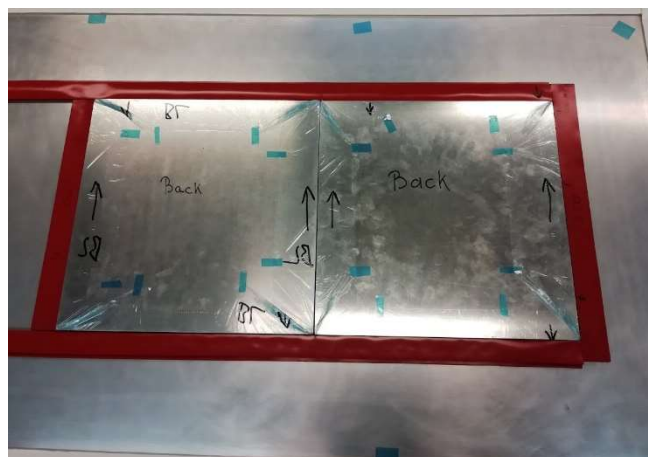
Fig. 12. Prepreg laminate tooling.

After the lay-up and vacuum bagging processes, the tool plate was ready to be placed in the autoclave. Two vacuum hoses were connected to the bag, one for sustaining the vacuum and one for monitoring the pressure. I also connected three J-type thermocouples, one on each laminate, and one on the tool plate to monitor the temperature during the curing cycle. Now the laminates were ready for curing according to a cycle based on the prepreg manufacturer's recommendation: 7 bar and 125°C for 60 min.

Fig. 13. The tool plate with the laminates in the autoclave.

After completion of the curing cycle, the composite plates were removed from the autoclave and demoulded from the tool plate. The burr was cleaned from the edges and removed small bumps from the sides with sandpaper. The laminates were then cut into the desired shape and size in two different directions with a diamond cutting wheel on a Mutronic Diadisc 5200 type machine. The nominal dimensions of the finished specimens were 150x100x4 mm. After cutting, I cleaned the specimens of dust and marked them. The labelling was BL for baseline laminate and M for the laminate modified with release film, 0 for the 0° middle plies orientation and 90 for the 90° middle plies orientation.

3.5.2. Quasi-Static Indentation Test

The test method for measuring the damage resistance of the prepreg composites to a concentrated quasi-static indentation force was based on the ASTM D6264/D6264M standard [5]. For support, I used the drop weight impact support fixture (Fig. 14.) which was made based on the ASTM D7136/D7136M standard [16], for good comparability in further investigations using the drop-weight impact test method. For the same reason, the specimen geometry was 150x100x4 mm based on the compression after impact standard. The diameter of the hemispherical indenter tip was 16 mm.

Fig. 14. Static Indentation test setup with camera and backlights.

I tested the 1BL0, 5BL90, 3M0, and 5M90 specimens with 2.5 mm/min test speed until final failure and stopped recording data when the force decreased under 5 kN. This way I became aware of the shape of the full force-displacement curve for all the specimen types. I tested the 2BL0, 4BL90, 2M0, and 4M90 specimens with 2.5 mm/min test speed until 8 mm displacement. This way I could stop the test before the first big load drop and later examine the damage introduced into the specimens with a non-destructive test method. After the non-destructive testing (see section 3.5.3) I re-loaded the same specimens to the same displacement with 4 mm/min test speed to assess their stiffness degradation often used as a damage parameter. In fact, the specimens had about 1 mm permanent deformation which I did not consider when setting up the test machine for the re-loading test. Therefore, the specimens were loaded up to about 9 mm total indentation which introduced further damage. I tested the 3BL0, and 1M0 specimens with 2,5 mm/min test speed until 7 mm indenter displacement. Based on previous experiences, this amount of displacement caused an adequate amount of damage and made the specimens relevant for later mechanical testing (3.5.4). I re-loaded the specimens with 5 mm/min test speed until 6 mm indenter displacement to assess their stiffness degradation without introducing further damage.

Table 3. Static indentation test parameters.

Sequence	Specimen type			Test Speed [mm/min]	Max. Indenter Displacement [mm]	Comment
	BL	M	[°]			
1	1BL0	3M0	0	2.5	N/A	Until final failure
	5BL90	5M90	90			
2	2BL0	2M0	0	2.5	8	Stopped before first load drop
	4BL90	4M90	90			
3	2BL0	2M0	0	4	9	Re-load
	4BL90	4M90	90			
4	3BL0	1M0	0	2.5	7	Damage introduction
	-	-	-			
5	3BL0	1M0	0	5	6	Re-load
	-	-	-			

I used the following equations to evaluate the numerical results.

$$E_{F_{max}} = E(\delta_{F_{max}}) = \int_0^{\delta_{F_{max}}} F(\delta)d\delta$$

where:

δ = indenter displacement, [mm] ,

$\delta_{F_{max}}$ = indenter displacement at maximum contact force, [mm] ,

$F(\delta)$ = measured contact force at indenter displacement δ, [N],

F_{max} = measured maximum contact force, [N],

$E(\delta)$ = energy until displacement δ, [J], and

$E_{F_{max}}$ = absorbed energy until indenter displacement at maximum contact force, [J].

$$E_{total} = E(\delta_{max}) = \int_0^{\delta_{max}} F(\delta)d\delta$$

where:

δ_{max} = maximum indenter displacement, [mm], and

E_{total} = absorbed energy until maximum indenter displacement, [J]

3.5.3. X-CT scan

The 2BL0, 4BL90, 2M0 and 4M90 specimens which were damaged previously by indentation until 8 mm displacement, were examined with X-ray computed tomography (CT). The scanning was carried out at Széchenyi István University. The examination of the four specimens happened in one operation on a Yxlon Modular CT machine with conical beam and 2048x2048 pixel flat panel detection at 225 kV tube voltage. VolumeGraphics StudioMax software was used for the reconstruction of the data.

3.5.4. Compression After Indentation Test

The test method for measuring the compressive residual strength properties of damaged polymer matrix composite plates was conducted according to the standard ASTM D7137/D7137M [13]. I used the compressive residual strength support fixture (Fig. 15.). I aligned the compression platens in a parallel position. I applied 450 N compressive force to the fixture assembly with the specimen each time after mounting the test panel, to ensure all loaded surfaces were in sufficient contact, then returned to the start position. I also applied 150 N pre-load before starting data acquisition with the test machine. The crosshead displacement rate was 1 mm/min in all cases. I tested the 2BL0, 4BL90, 2M0, 4M90 and 3BL0, 1M0 specimens which were damaged previously by indentation test (9 and 7 mm indentation).

Fig. 15. Compression after indentation test setup with camera and backlight.

I used the following equations to evaluate the test results.

$$\sigma_{CAI} = F_{max}/A$$

Where σ_{CAI} = ultimate compressive residual strength, [MPa], F_{max} = maximum force before failure, [N], A = cross-sectional area = $h \cdot w$, [mm^2], h and w are the thickness and the width of the test panels.

16

3.5.5. *Video recording*

I made video recordings of the static indentation and compression after impact tests. The first attempts were recording the back face of a specimen during an indentation test with a conventional mobile phone camera. Then I used bright lights to illuminate the specimens' front face and make a backlight effect occur on the other side. As it showed useful and interesting images, I decided to switch to a professional high-resolution camera and used that in the following tests. The 5 Mpixel Mercury Monet camera was originally supplied with our digital image correlation-based video-extensometer system, but it was suitable for our simple recording purpose as well.

4. RESULTS AND DISCUSSION

4.1. Quasi-Static Indentation Test

The contact force versus indenter displacement curves from the first series of indentation tests (1BL0, 5BL90, 3M0, 5M90) carried out until final specimen failure are shown in Fig. 16.
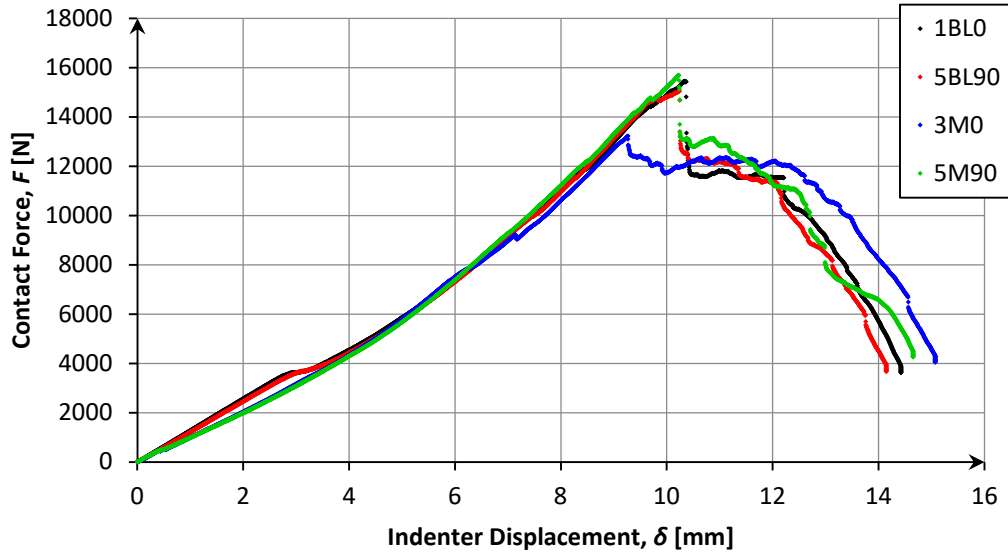
Fig. 16. Force-displacement curves of the specimens loaded until failure.

Table 4. Numerical results of the first series of indentation tests.

Specimen			Maximum Contact Force [kN]	Energy Until Maximum Contact Force [J]	Tolal Absorbed Energy [J]
Type	[°]	Label			
BL	0	1BL0	15,4	71,1	110,5
	90	5BL90	15,0	69,0	106,9
M	0	3M0	13,2	53,0	114,4
	90	5M90	15,7	68,3	111,8

I compared the specimens as a baseline (BL) to modified (M) and 0° to 90°. Investigating the specimens which were loaded until final failure the following observation can be made.

Regarding the 0° specimens (1BL0, 3M0) the baseline specimen had a 15.5% higher maximum contact force and required significantly (29.2%) higher energy to reach it. In terms of total energy absorption (until the force decreased under 5 kN), the baseline and modified specimen had similar results (only 3.6% difference). However, in the modified case, there was a significant difference: plateau instead of peak for the 0 degree.
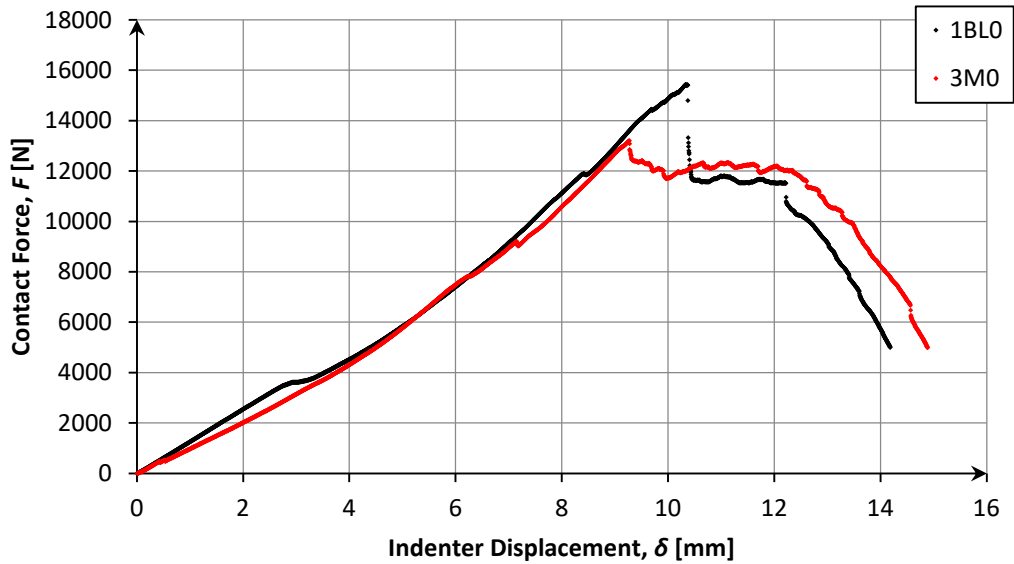
Fig. 17. Force-displacement curves for specimens loaded until failure.

Regarding the 90° specimens (5BL90, 5M90) the modified specimen had slightly higher maximum contact force and total energy absorption (4.2% and 5.1% difference). These specimens required about the same total energy to reach the maximum contact force (1% difference).
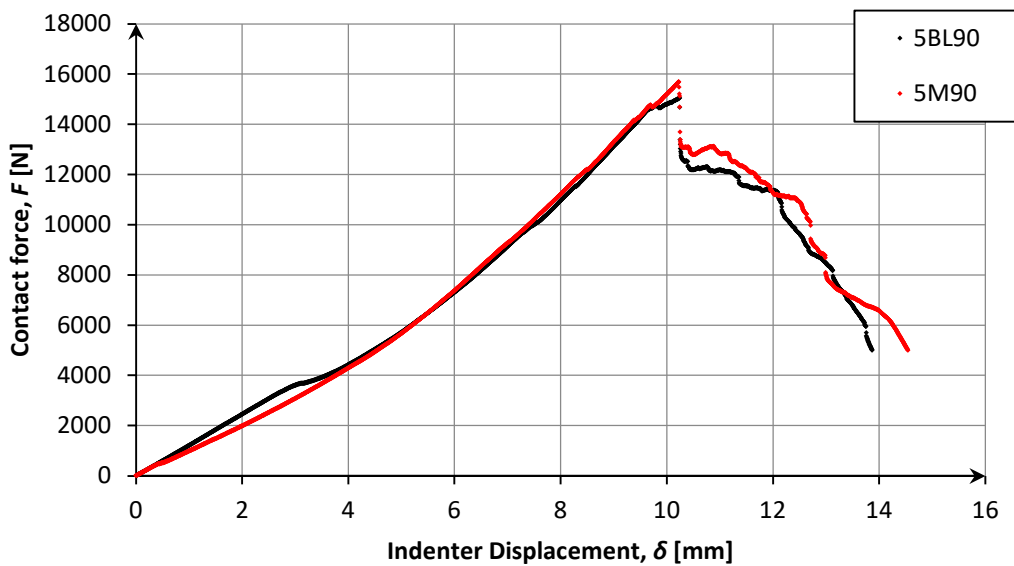
Fig. 18. Force-displacement curves for specimens loaded until failure.

Comparing 0° and 90°, within the baseline type (1BL0, 5BL90), the 0° specimen reached slightly higher values, but the differences were not significant. In the case of the baseline specimens, no difference was found in the shape of the curves for the 0- and 90-degree specimens.

19
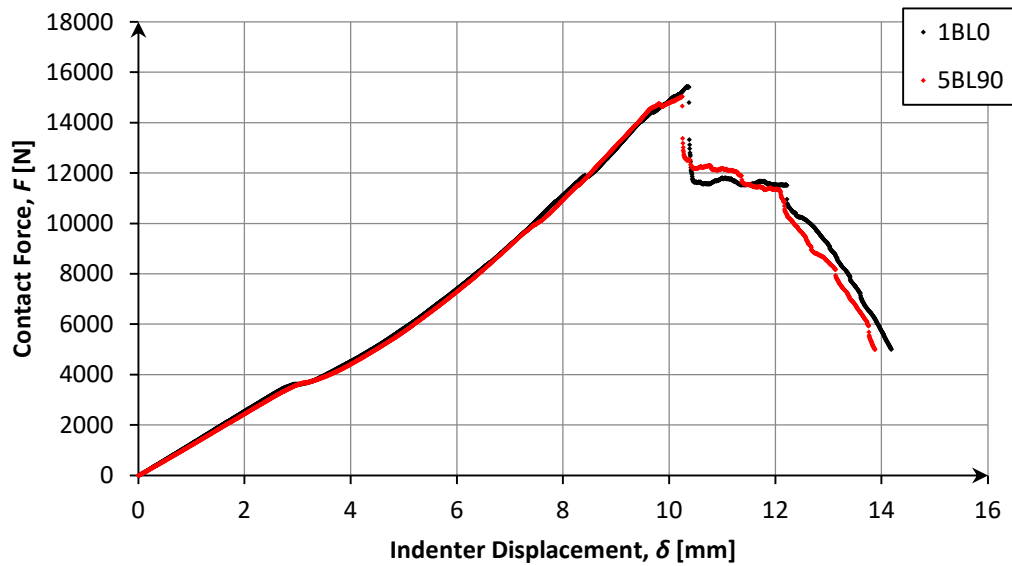
Fig. 19. Force-displacement curves for specimens loaded until failure.

The modified specimens cut out in different directions (3M0, 5M90) had significant differences. The 90° specimen had a higher maximum contact force and required more energy to reach it with a 17.1% and 25.3% difference respectively, while their total energy absorption was nearly equal (2% difference).
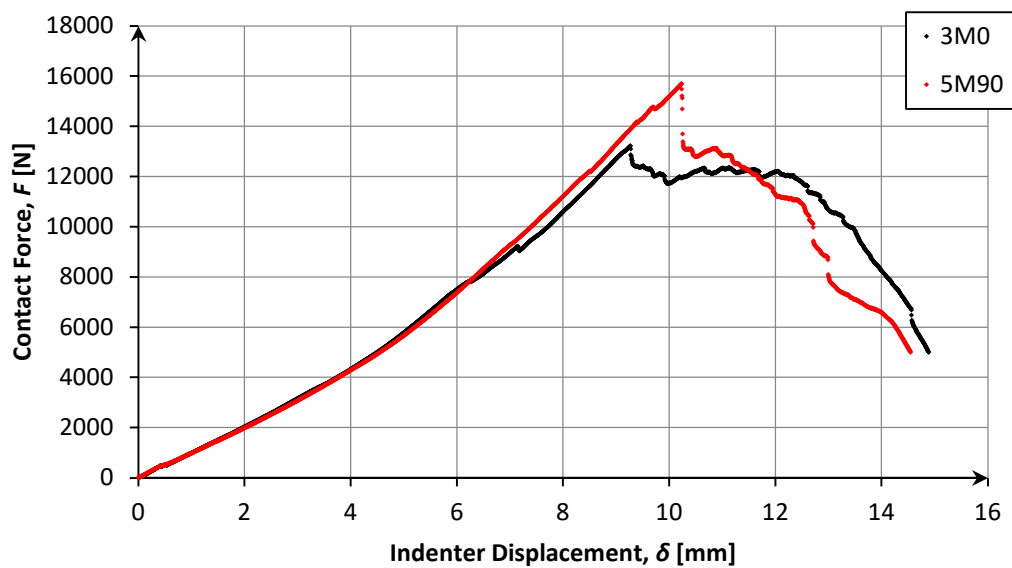
Fig. 20. Force-displacement curves for specimens loaded until failure.

The contact force versus displacement curves from the second series of indentation tests (2BL0, 4BL90, 2M0, and 4M90) in which specimens were loaded until 8 mm displacement to introduce similar extent of damage to them, are shown in Fig. 21.
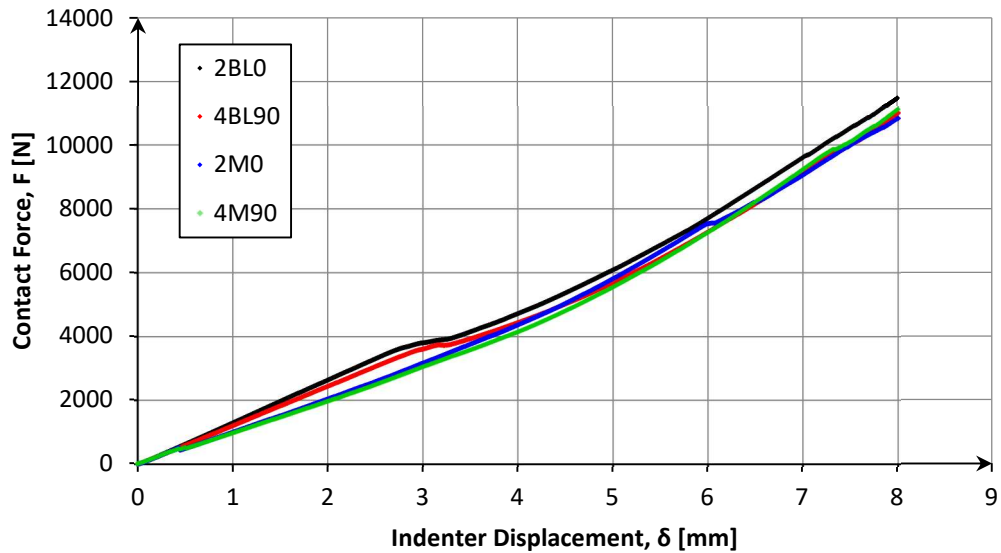
Fig. 21. Force-displacement curves for specimens loaded until 8 mm indentation.

It is interesting to note that the 0 degree specimens are slightly stiffer in both BL and M. This is possibly because in these specimens the shorter side is parallel to the fibres at 90 degrees, which are further away from the mid-plane, resulting in higher bending stiffness in this dominant direction.

The contact force versus displacement curves from the third series of indentation tests (2BL0, 4BL90, 2M0, 4M90) in which specimens were re-loaded to assess their stiffness reduction indicative of internal damage are shown in Fig. 22.
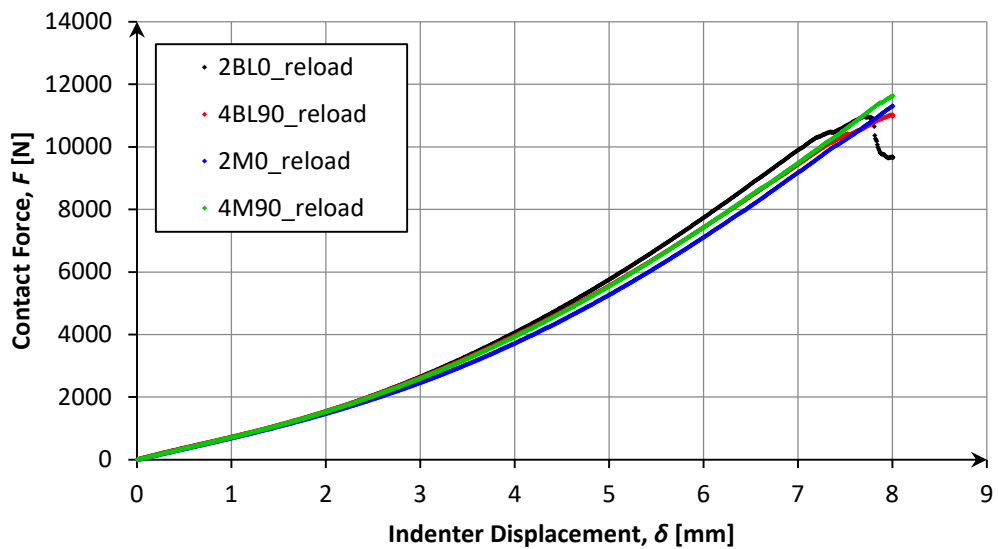
Fig. 22. Force-displacement curves for specimens reloaded until 9 mm indentation.

Table 5. Test specimens' stiffness and its change upon reload.

	First-load stiffness [N/mm]	Re-load stiffness [N/mm]	Difference [%]
2BL0	1328	758	**54.6**
4BL90	1224	752	**47.9**
2M0	1015	733	**32.2**
4M90	972	759	**24.6**

The contact force versus displacement curves from the indentation test of 3BL0 and 1M0 specimens are shown in Fig. 23.
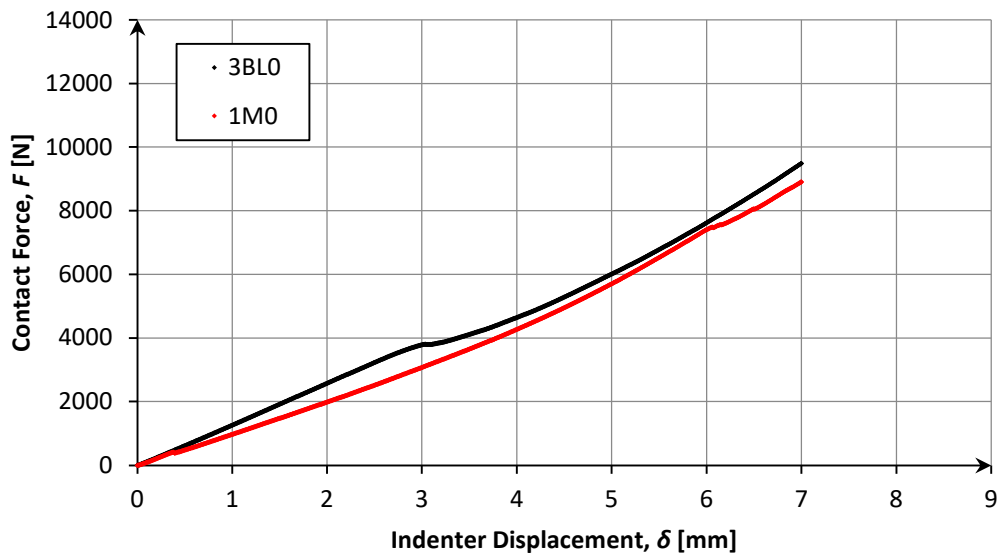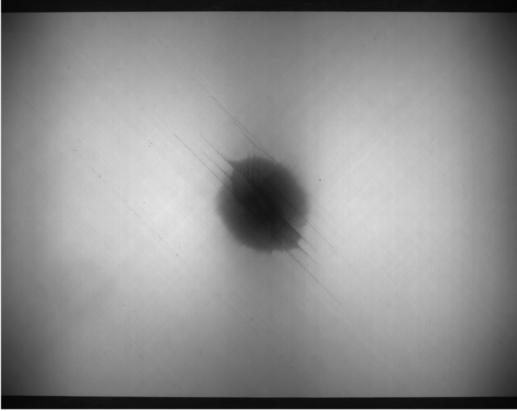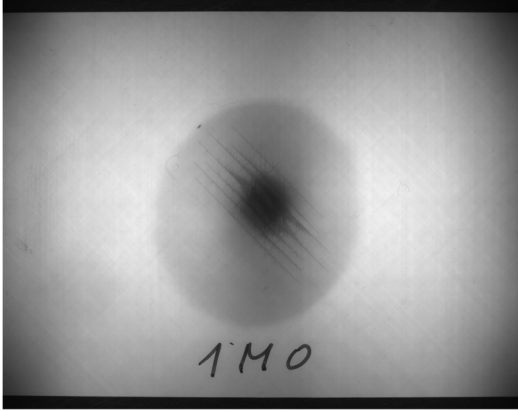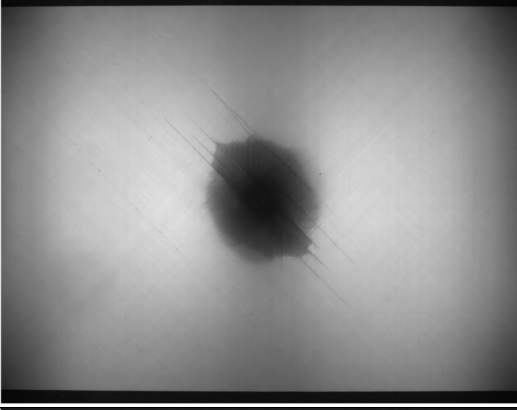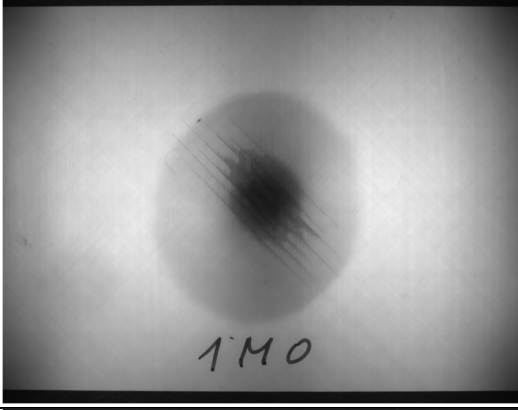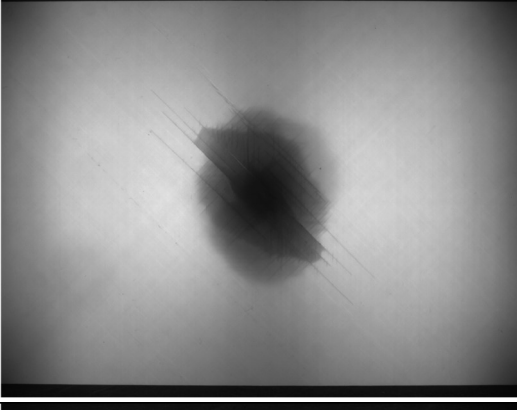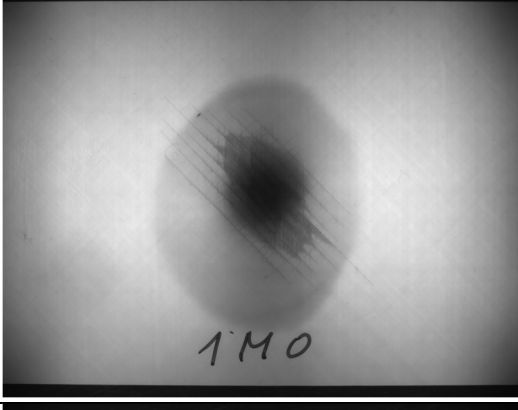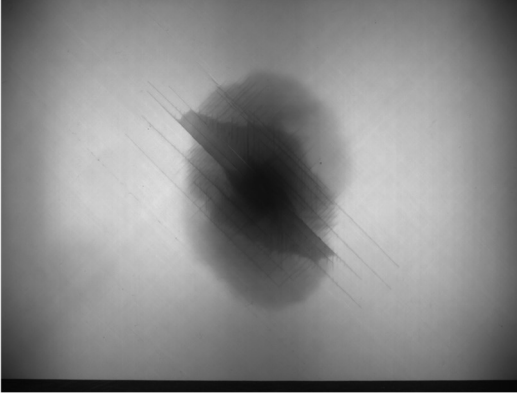

Fig. 23. Force-displacement curves for specimens loaded until 7 mm indentation.

Fig. 24. Images recorded during indentation tests (continued the next page)

δ [mm]	Specimen type	
	BL 0	M 0
0		
1		
2		
3		

δ [mm]	Specimen type	
	BL 0	M 0
4		
5		
6		
7		

The contact force versus displacement curves from the reloading indentation test of 3BL0 and 1M0 specimens are shown in Fig. 25.
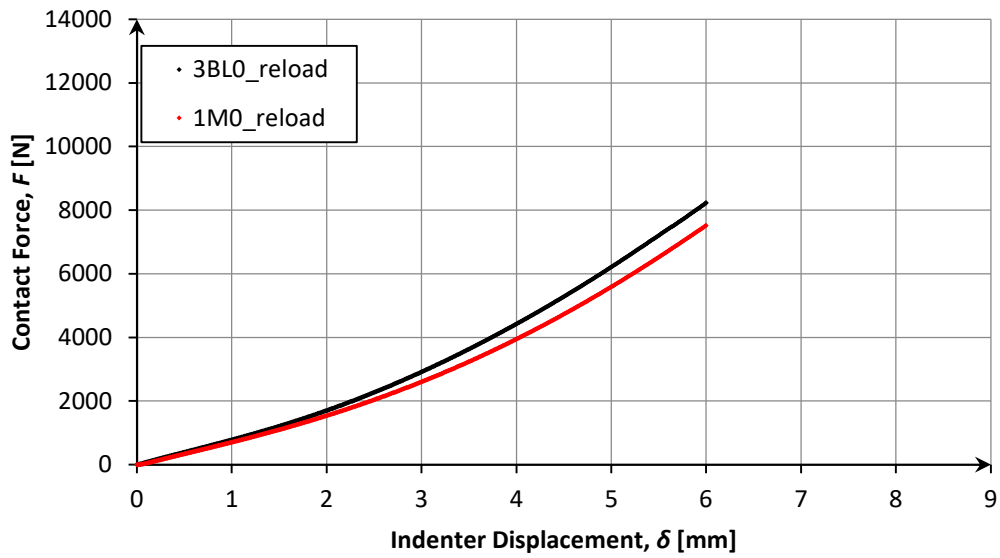

Fig. 25. Force-displacement curves for specimens re-loaded until 6 mm indentation.

I noticed, that the BL and M specimens previously had almost identical stiffness when reloaded. The behaviour of the samples does not seem to be perfectly reproducible.
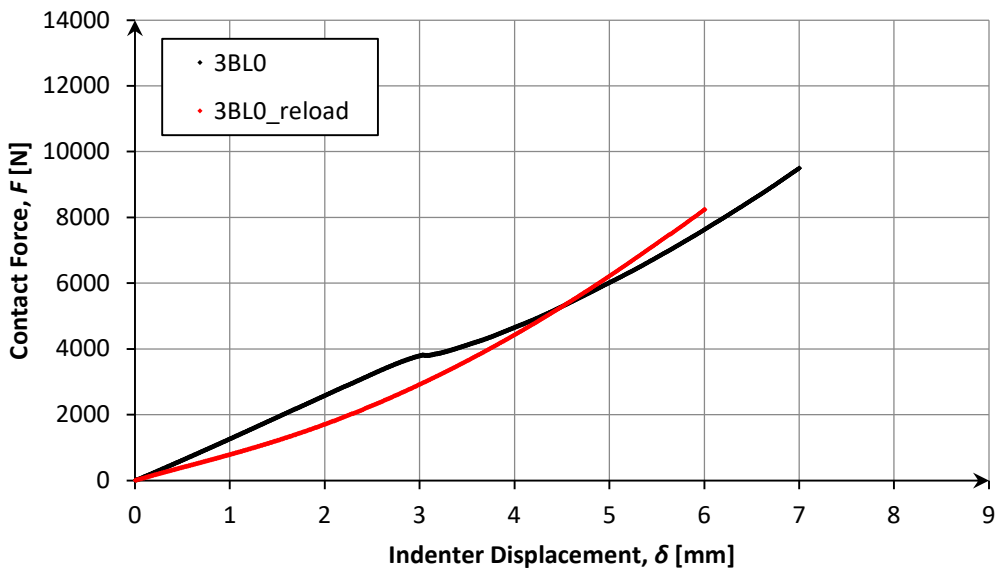

Fig. 26. Force-displacement curves of a specimen loaded (damaged) and re-loaded
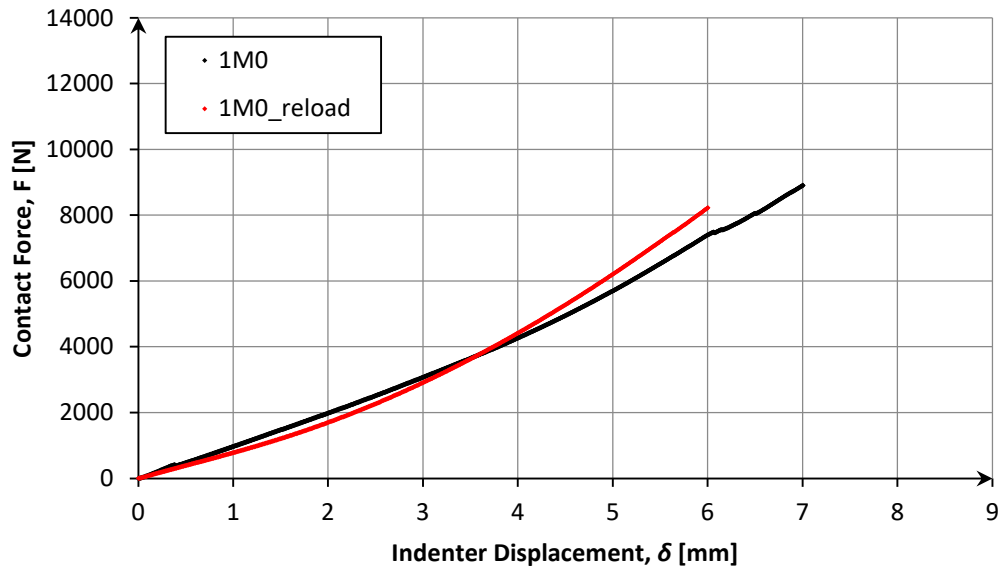
**Fig. 27.** Force-displacement curves of a specimen loaded (damaged) and re-loaded

The reduction in stiffness observed in the figures is shown numerically in Table 4.

Table 6. The change in stiffness between first- and re-load

	First-load stiffness [N/mm]	Re-load stiffness [N/mm]	Difference [%]
3BL0	1294	843	**42.2**
1M0	991	771	**24.9**

4.2. X-CT scan

The X-CT scan of 2BL0, 4BL90, 2M0, and 4M90 specimens which were previously damaged by 8 mm indentation are shown in **Fig. 28**. Due to the width of the test specimens, the resolution of the scan images did not allow detailed analysis. However, I managed to observe a general trend: baseline specimens show delamination at more interface than the modified specimens.
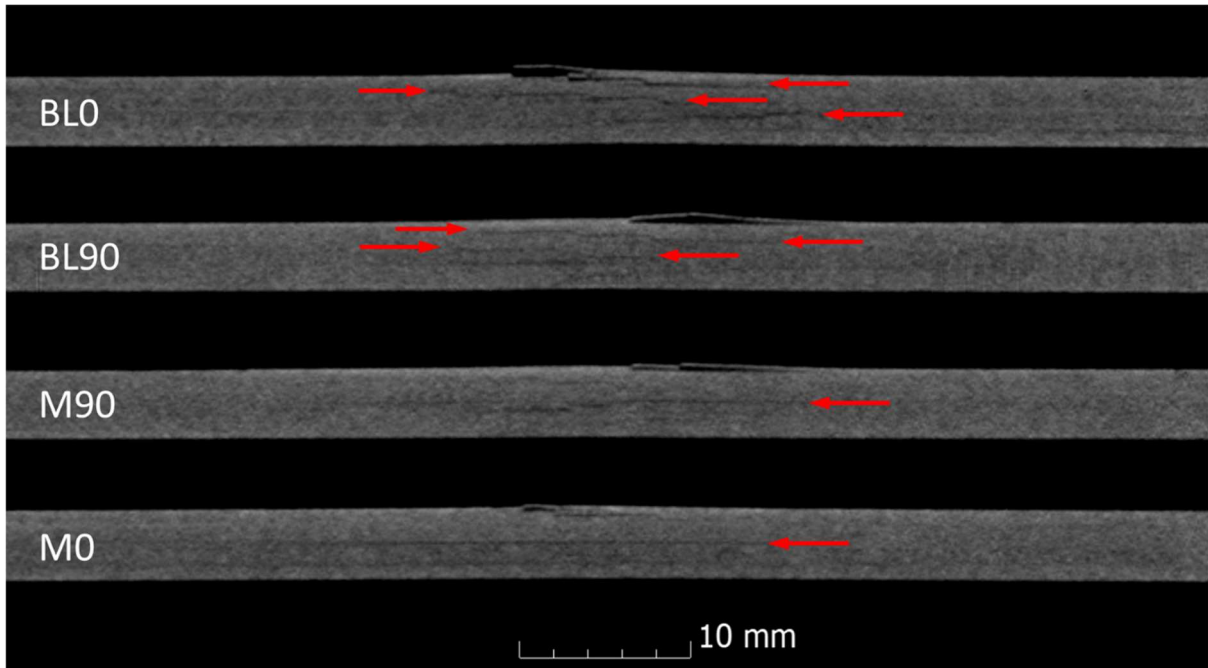
Fig. 28. The X-CT scan cross-section image of specimens damaged by 9 mm indentation.

4.3. Compression After Indentation Test Results

The stress versus strain curves from the compression after indentation (CAI) tests of all tested specimens are shown in Fig. 29.
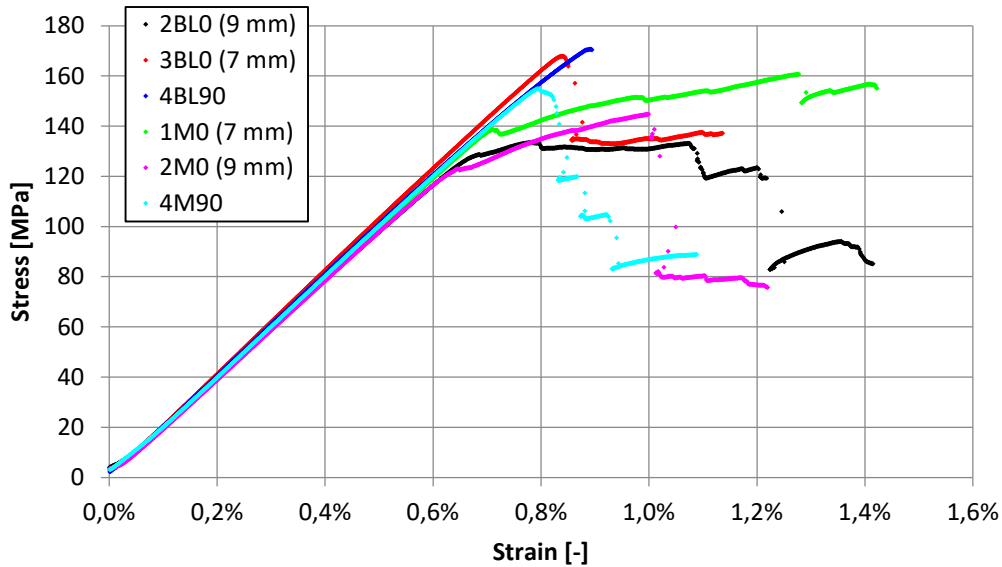

Fig. 29. Stress-strain curves for specimens loaded until failure in compression after indentation (CAI). (Numbers in brackets in the specimen designations indicate damage extent.)

Comparing the baseline and modified specimens, the following can be stated. From the 0° specimens those which were indented until 8 mm (2BL0, 2M0) the ultimate residual strength of the modified specimen was higher, with an 8.1% difference, but its total energy absorption was lower, with a 21.1% difference.
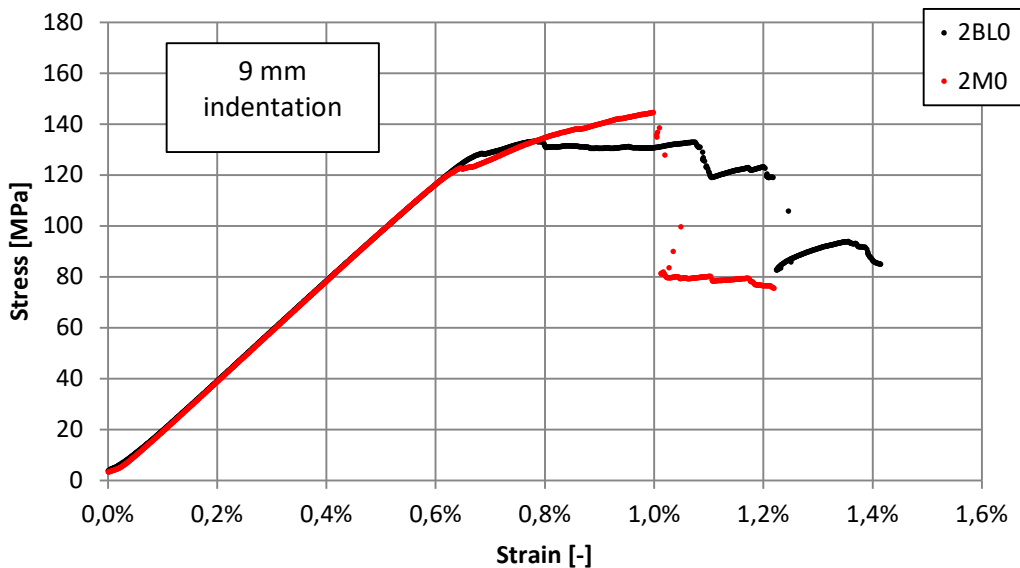

Fig. 30. CAI stress-strain curves for specimens damaged until 9 mm indentation.

The plates indented only until 7 mm displacement, (3BL0, 1M0) the modified specimen reached 4.3% lower ultimate residual strength and had 31.8% higher total energy absorption.
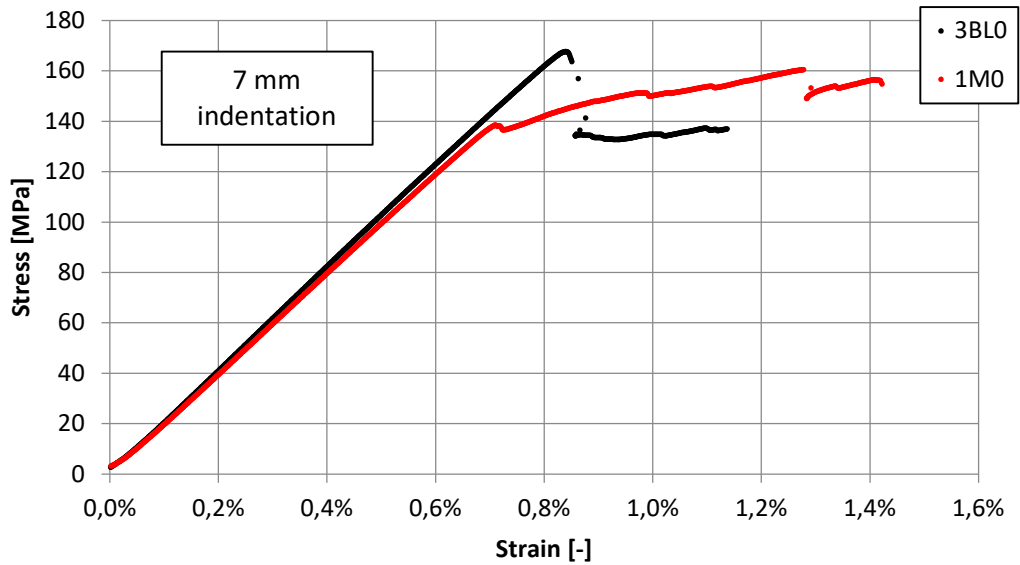

Fig. 31CAI stress-strain curves for specimens damaged until 7 mm indentation.

From the 90° specimens which were indented until 9 mm (4BL90, 4M90) the modified specimen showed lower values in every aspect. The difference was 9.6% for the ultimate residual strength and 9.9% for the total energy absorption.
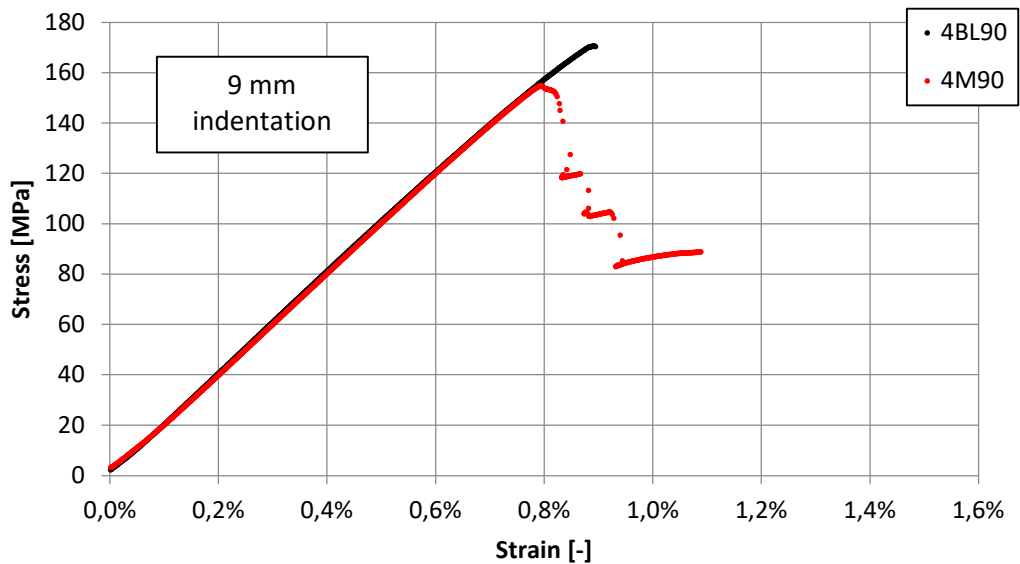

Fig. 32. CAI stress-strain curves for specimens damaged until 9 mm indentation.

In the following, I compared the 0° and 90° specimens. Both the baseline and the modified 90° specimens had higher ultimate residual strength (24.4% and 6.8% diff) but lower total energy absorption (25.6% and 14.4%). This means that they generally exhibited a stronger, but more brittle behaviour.
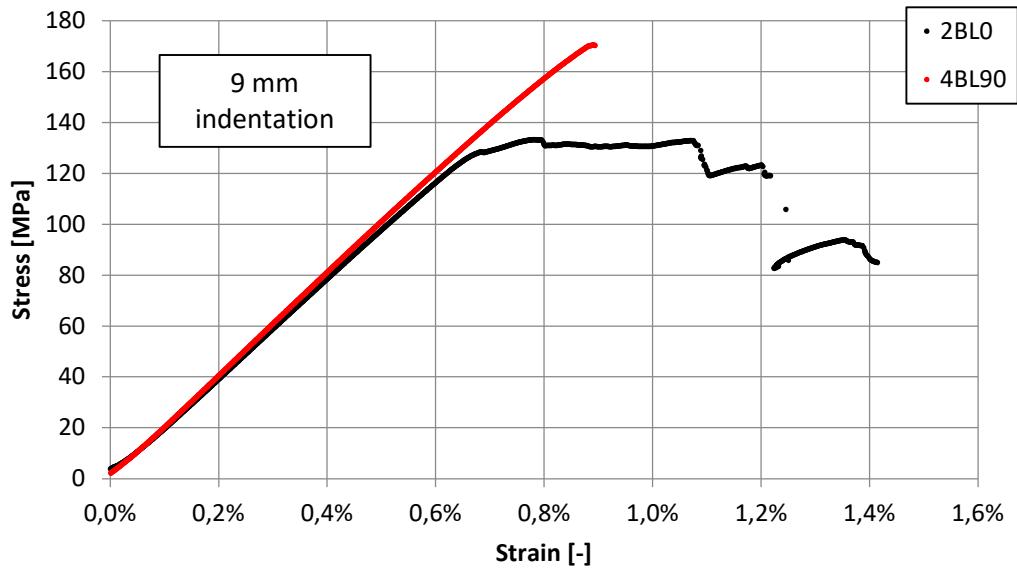

Fig. 33. CAI stress-strain curves for specimens damaged until 9 mm indentation.
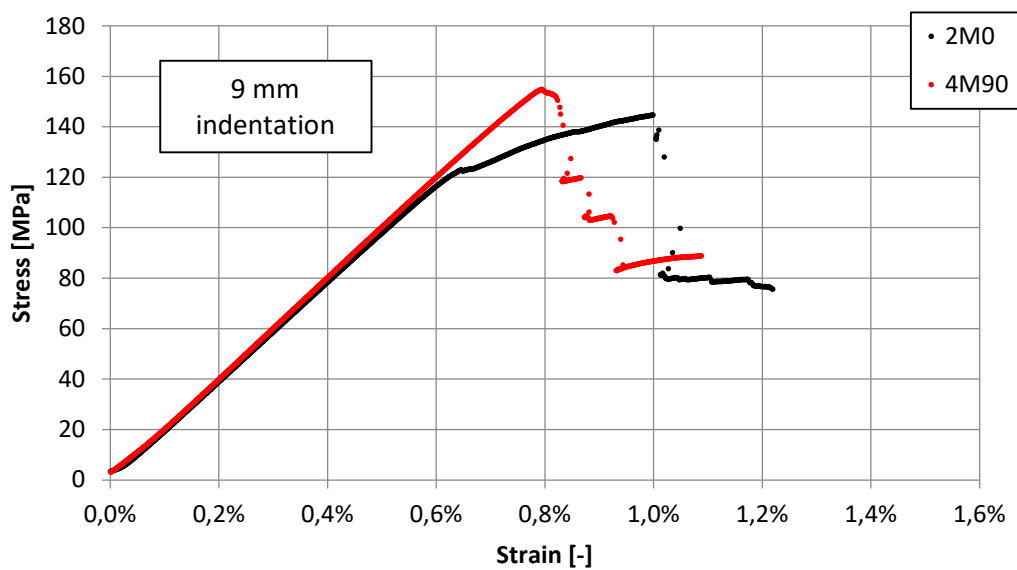

Fig. 34. CAI stress-strain curves for specimens damaged until 9 mm indentation.

Finally, I investigated the effect of the induced damage. In both the baseline and the modified cases, those specimens which were damaged by less severe indentation (3BL0, 1M0) performed better in every aspect. The difference was 22.8% and 10.5% in ultimate residual strength, and 5.0% and 52.6% in total energy absorption.

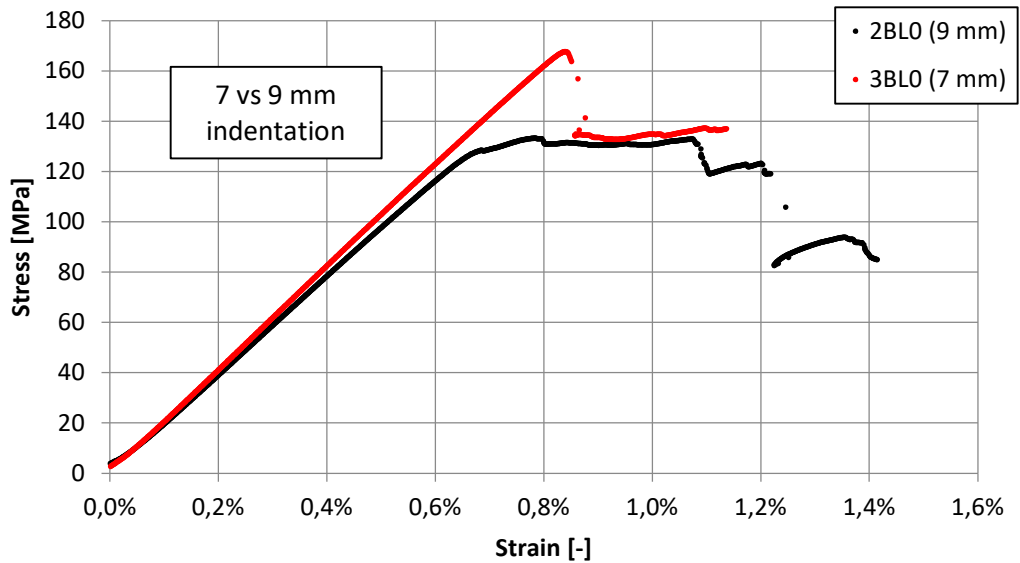**Fig. 35.** CAI stress-strain curves for specimens damaged until 7- and 9-mm indentation.
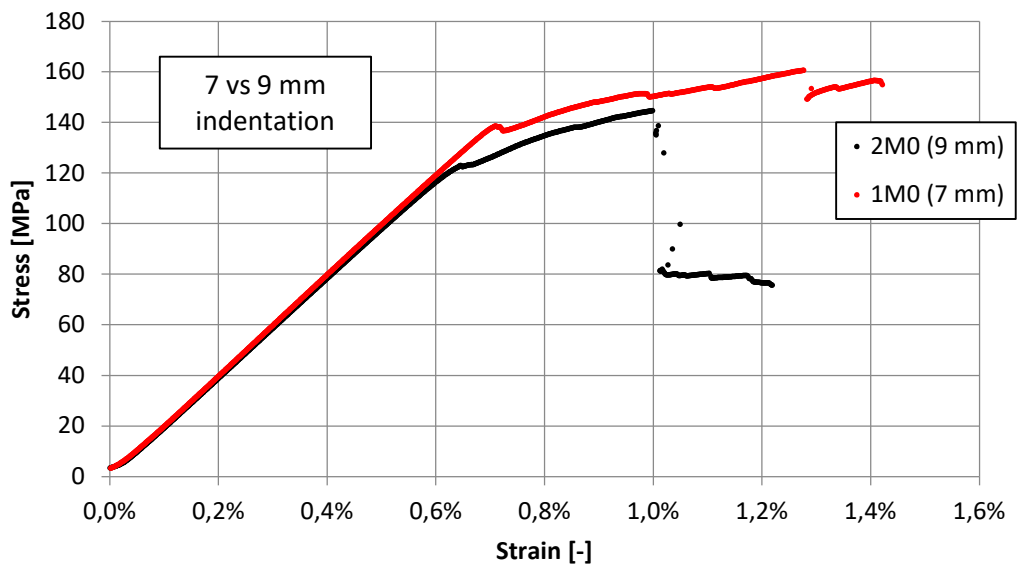

Fig. 36. CAI stress-strain curves for specimens damaged until 7- and 9-mm indentation.

Figures 37 and 38 show the image series recorded during the CAI tests. These will serve as a basis for further damage and failure evaluation in the future.
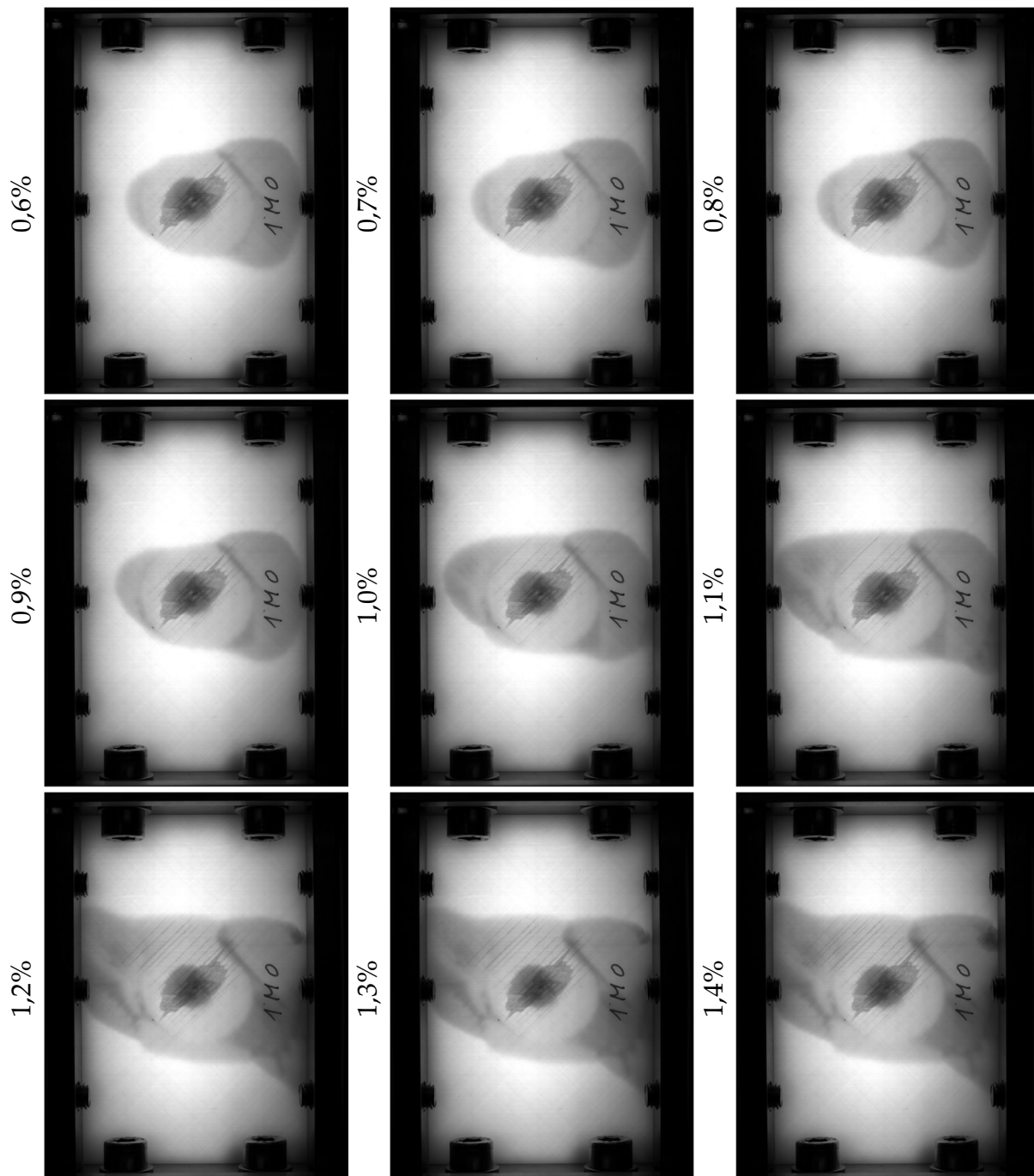
Fig. 37. Images recorded during compression after indentation test with strain labels.

| | 0,6% | 0,7% | 0,8% |

| | 0,9% | 1,0% | 1,1% |
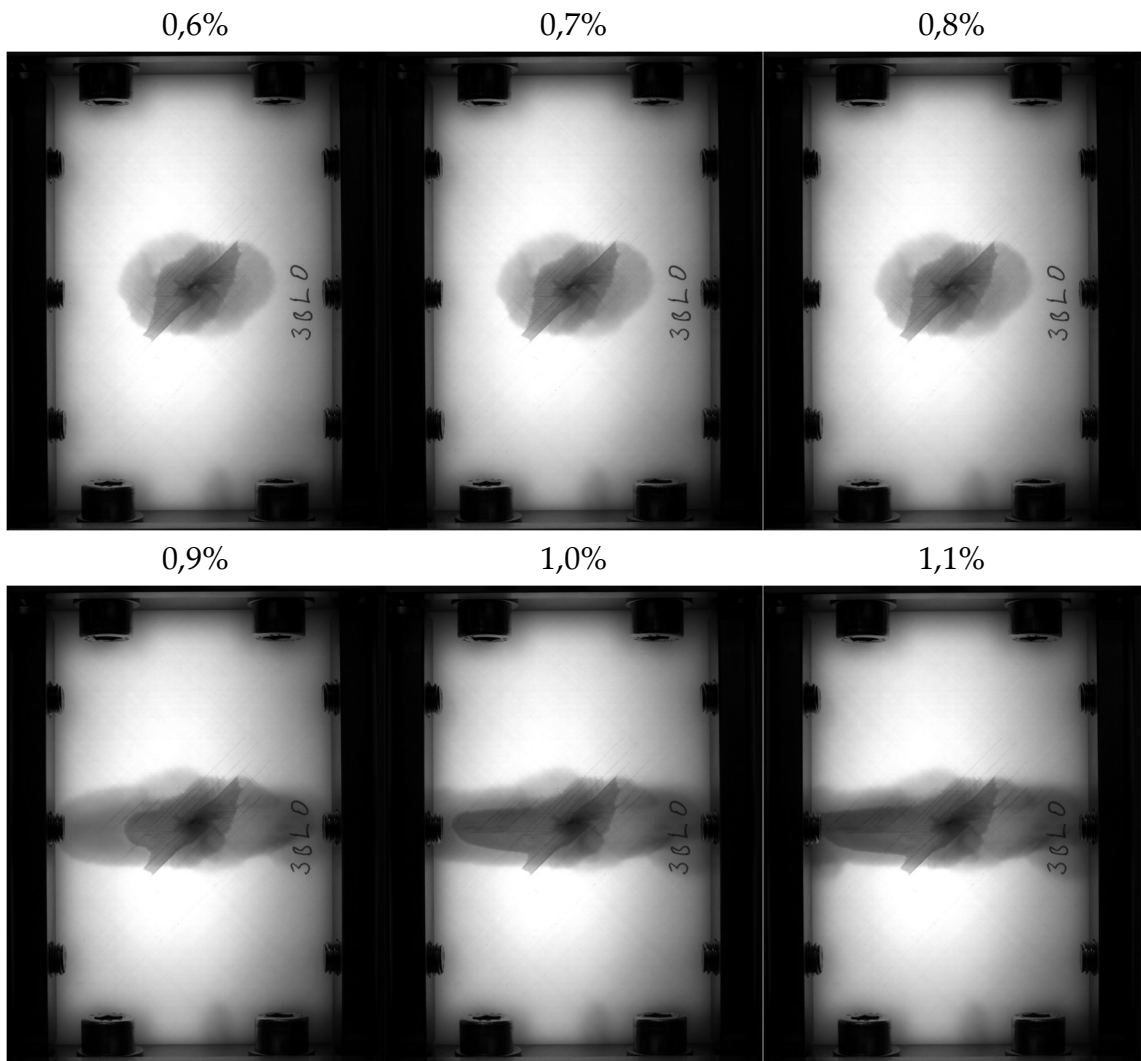
Fig. 38. Images recorded during compression after indentation test with strain labels.

Table 7 shows the CAI test results for reference.

Table 7. Test results of the CAI experiments

Spec. designation	Indentation damage [mm]	Effective modulus [GPa]	CAI strength [MPa]	Total absorbed energy [J]
2BL0	9	19,6	134	86,2
4BL90	9	20,3	171	48,4
2M0	9	19,7	145	71,9
4M90	9	20,0	155	56,8
3BL0	7	20,7	168	72,6
1M0	7	20,0	161	95,9

5. CONCLUSION

I fabricated quasi-isotropic S-glass/epoxy prepreg composite laminates. Then produced modified versions with circular PTFE release film interleaves were placed in the middle interlayer. I have carried out quasi-static indentation tests with various parameters. Then examined the damaged specimens with computed tomography scanning. The previously damaged specimens were further investigated with compression after indentation tests. I recorded the mechanical tests with a high-resolution camera while the specimens were illuminated from the other side with strong light. The following observations were made:

- The fibre orientation makes a notable difference upon quasi-static indentation and compression after impact tests.
- The delamination failure mechanism dominated during the first stages of damage introduction.
- The delamination of plies occurred at several interfaces at the same time and migrated through the interlayers especially in case of the baseline plates.
- The delamination damage of the interleaved interface appeared at low displacement over the inserted release film and increased during loading. The modified laminates showed no plateau in the load-displacement curve observed for the baseline plates under quasi-static indentation.
- The laminates without interleaves showed a plateau in the force-displacement curve which had a notable effect on further load-bearing. Further investigation is needed to identify the responsible damage mode.
- The modification with release film did not decrease the total energy absorption upon quasi-static indentation.
- The resolution of the CT-scans was insufficient due to the 100 mm width of the scanned samples; therefore, it was hard to draw conclusions from them.
- The processing of CT-scan recordings requires the use of advanced software and expertise.
- Widely available optical equipment can be used to make useful real-time observations of the damage process inside the laminate and to later analyse what happened.
- This method provides not as detailed information as a C-scan or CT-scan but shows information in real-time and does not require complex and expensive equipment.

REFERENCES

[1] S. G. Marino and G. Czél, 'Development and characterisation of reparable, film-interleaved, pseudo-ductile hybrid composites', *Compos Part A Appl Sci Manuf*, vol. 169, p. 107496, Jun. 2023, doi: 10.1016/J.COMPOSITESA.2023.107496.

[2] A. Cohades, C. Branfoot, S. Rae, I. Bond, and V. Michaud, 'Progress in Self-Healing Fiber-Reinforced Polymer Composites', *Advanced Materials Interfaces*, vol. 5, no. 17. Wiley-VCH Verlag, Sep. 07, 2018. doi: 10.1002/admi.201800177.

[3] S. G. Marino, F. Mayer, A. Bismarck, and G. Czél, 'Effect of Plasma-Treatment of Interleaved Thermoplastic Films on Delamination in Interlayer Fibre Hybrid Composite Laminates', *Polymers 2020, Vol. 12, Page 2834*, vol. 12, no. 12, p. 2834, Nov. 2020, doi: 10.3390/POLYM12122834.

[4] E. Abisset, F. Daghia, X. C. Sun, M. R. Wisnom, and S. R. Hallett, 'Interaction of inter- and intralaminar damage in scaled quasi-static indentation tests: Part 1 – Experiments', *Compos Struct*, vol. 136, pp. 712–726, Feb. 2016, doi: 10.1016/J.COMPSTRUCT.2015.09.061.

[5] 'Standard Test Method for Measuring the Damage Resistance of a Fiber-Reinforced Polymer-Matrix Composite to a Concentrated Quasi-Static Indentation Force 1', doi: 10.1520/D6264_D6264M-17.

[6] Y. S. Kwon and B. V. Sankar, 'Indentation-Flexure and Low-Velocity Impact Damage in Graphite Epoxy Laminates', *Composites Technology and Research*, vol. 15, no. 2, pp. 101–111, Jun. 1993, doi: 10.1520/CTR10361J.

[7] S. Abrate, 'Impact on Composite Structures', *Impact on Composite Structures*, Apr. 1998, doi: 10.1017/CBO9780511574504.

[8] S. Guinard, O. Allix, D. Guédra-Degeorges, and A. Vinet, 'A 3D damage analysis of low-velocity impacts on laminated composites', *Compos Sci Technol*, vol. 62, no. 4, pp. 585–589, Mar. 2002, doi: 10.1016/S0266-3538(01)00153-1.

[9] Y. Gao, W. Hu, S. Xin, and L. Sun, 'A review of applications of CT imaging on fiber reinforced composites', *Journal of Composite Materials*, vol. 56, no. 1. SAGE Publications Ltd, pp. 133–164, Jan. 01, 2022. doi: 10.1177/00219983211050705.

[10] D. J. Bull, S. M. Spearing, and I. Sinclair, 'Observations of damage development from compression-after-impact experiments using ex situ micro-focus computed tomography', *Compos Sci Technol*, vol. 97, pp. 106–114, Jun. 2014, doi: 10.1016/J.COMPSCITECH.2014.04.008.

[11] J. Jodhani, A. Handa, A. Gautam, Ashwni, and R. Rana, 'Ultrasonic non-destructive evaluation of composites: A review', *Mater Today Proc*, vol. 78, pp. 627–632, Jan. 2023, doi: 10.1016/j.matpr.2022.12.055.

[12] S. Guinard, O. Allix, D. Gue´drague´dra-Degeorges, and A. Vinet, 'A 3D damage analysis of low-velocity impacts on laminated composites'. [Online]. Available: www.elsevier.com/locate/compscitech

[13] 'Standard Test Method for Compressive Residual Strength Properties of Damaged Polymer Matrix Composite Plates 1', doi: 10.1520/D7137_D7137M-07.

[14] N. Zhang *et al.*, 'High-velocity impact damage and compression after impact behavior of carbon fiber composite laminates: Experimental study', *Int J Impact Eng*, vol. 181, Nov. 2023, doi: 10.1016/j.ijimpeng.2023.104749.

[15] 'http://www.pt.bme.hu/'.

[16] 'Standard Test Method for Measuring the Damage Resistance of a Fiber-Reinforced Polymer Matrix Composite to a Drop-Weight Impact Event 1', doi: 10.1520/D7136_D7136M-07.

[17] 'https://www.zwickroell.com/industries/composites/compression-after-impact-cai/'.